2014 IEEE International Conference on Control Applications (CCA)
Part of 2014 IEEE Multi-conference on Systems and Control
October 8-10, 2014. Antibes, France

Circulating Fluidized Bed Boiler State Estimation with an Unscented Kalman Filter Tool

M. Hultgren, E. Ikonen and J. Kovács

Abstract— **The paper discusses the development of a state estimation tool for circulating fluidized bed (CFB) boiler dynamic hotloop models. Bayesian state estimation was used to determine inputs, states and time-variant parameters based on output observations. The goal was to apply advanced state estimation to the original nonlinear model and utilize it for real-life CFB applications. The main algorithm of the tool was the unscented Kalman filter (UKF), with an SIR particle filter as a backup solution. The implementation of the tool and the UKF algorithm were described. The tool was tested with two simulation cases. In the first case, fuel flows and an air leakage parameter were identified based on flue gas compositions for pilot oxy combustion measurements. In the second case, heat transfer coefficient and fuel moisture content values were estimated in an industrial boiler based on the dense bed furnace temperature and the flue gas O_2 content. The results showed a good agreement between measurements and simulations, as well as a good computational performance for the UKF.**

I. Introduction

The use of modern state estimation methods in circulating fluidized bed (CFB) power plants is discussed in this paper. Models used for process control typically have relatively simple structures [1], such as transfer function or input response models. More complex models are used in process design. As these models are often at least partially based on process knowledge, they are larger and heavier to run, with many states and equations to be solved. There is an increasing interest towards utilizing these models also for control purposes. This development is driven by the continuous increase in available computing power.

Deviations between simulated and measured outputs can be attributed to an insufficient model, measurement or input inaccuracies and unmeasured disturbances during test periods. As power plant experiments are typically expensive and time-consuming to conduct, measurements with inaccuracies, noise and disturbances often have to be used for model validation and design. Bayesian state estimation enables an effective utilization of this data in a stochastic framework. By estimating unmeasured states and time-varying parameters (e.g. fuel quality, gas flows, fouling), observed outputs can be explained through changes in the process or its inputs. Information about e.g. heat transfer coefficients is also required during process modeling. In control, state estimation is mainly utilized for filtering (e.g. Kalman filters), state observers and monitoring.

M. Hultgren and E. Ikonen are with the Systems Engineering Laboratory, University of Oulu, Oulu, CO 90014 Finland (phone: +358 50 350 2923; fax: +358 8 553 2304; e-mail: firstname.lastname@oulu.fi).

J. Kovács is with Foster Wheeler Energy Ltd, Varkaus, CO 78201 Finland (e-mail: jeno.kovacs@fwfin.fwc.com).

This paper describes the development of a Bayesian state estimation tool for a dynamic CFB simulator. The main goal was to apply advanced state estimation techniques to the existing nonlinear model. The unscented Kalman filter (UKF) was selected as the main algorithm for the tool due to its reported performance [2,3]. An additional goal was to show, how state estimation can be used in CFB engineering. To this end, two simulation cases were studied. In the first case, fuel flows and an air leakage parameter were adjusted to reach a better agreement between measured and simulated flue gas compositions for pilot oxy combustion load ramp tests. In the second case, a furnace heat transfer coefficient and the time-varying fuel moisture content were estimated in an industrial boiler to reach the measured dense bed temperature and flue gas O_2 content.

While the unscented Kalman filter is starting to become relatively well-known, the main contribution of this work is its implementation to a complex industrial CFB model. To the authors' knowledge, the UKF has not been applied in CFB boilers before, and its potential for solving estimation problems in this environment should be properly assessed before developing the algorithm further. State estimation work is scarce in the CFB field. Kalman, extended Kalman and H_∞ estimators were examined in [4,5] for a cold flow CFB, with the intention of determining the void fraction and bed height in the standpipe by measuring the pressure drop. A strong tracking filter was proposed in [6] to implement a furnace water-wall tube erosion monitoring system and to overcome the related robustness limitations of the extended Kalman filter. The particular state estimation problems of the current paper have not been addressed before (cf. preceding work [7]). The variations in the fuel moisture content and the heat transfer coefficients, the accuracy of reported fuel flows and the possibility of air leakage during oxy combustion are all important topics for CFB operation.

The CFB process and the used hotloop model are described in chapter II. The functionality of the hotloop state estimation tool and the principles of unscented Kalman filtering are explained in chapter III. Chapter IV gives an account of the state estimation tool simulations and their results. Chapter V sums up the conclusions of the work.

II. Process & Process Model

The circulating fluidized bed (CFB) boiler belongs to fluidized bed boilers, based on the combustion of solid fuels in a bed of incombustible material, e.g. sand or ash. The material is fluidized with the input gas flows, which contain the oxidizing agent needed for combustion. In the CFB configuration, solids become entrained with the gas flow and leave the furnace from the top, where they are separated

from the flue gas in gas-solid separators. The solids are then recycled back to the bed. Together, these process components form the CFB hotloop (Fig. 1).

The boiler heat exchangers for steam generation are located in the hotloop and the flue gas backpass, and they form the contact surface between the combustion side and the water-steam cycle of the boiler. The input oxidant in the CFB is typically air, but other oxidants can also be used. For example, in the oxy combustion carbon capture and storage (CCS) technology fuels are combusted with a mixture of pure oxygen and recirculated flue gas (RFG) instead of an air oxidant gas flow. This causes the CO_2 content to be elevated to 70–98 vol-% (dry) in the flue gas, enabling an easier separation and recovery of CO_2 emissions for storage [8].

The hotloop dynamics were modeled with a 1-D Matlab/Simulink model, which has been developed in cooperation between Foster Wheeler Energy Ltd, the Lappeenranta University of Technology and the University of Oulu. The model structure has been extensively validated and tested with various CFB boilers, and the model contains different process components depending on the boiler configuration (Fig. 2).

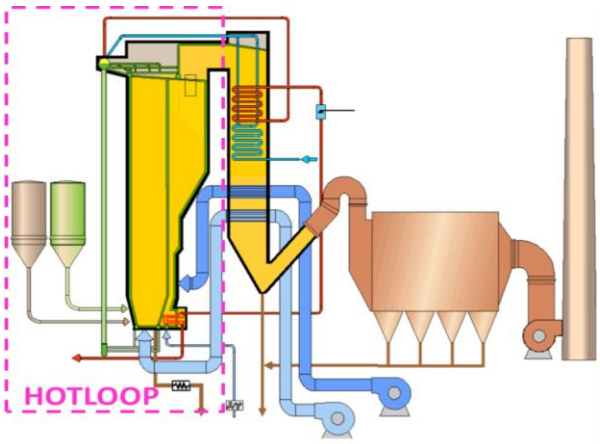

Figure 1. The circulating fluidized bed boiler hotloop.

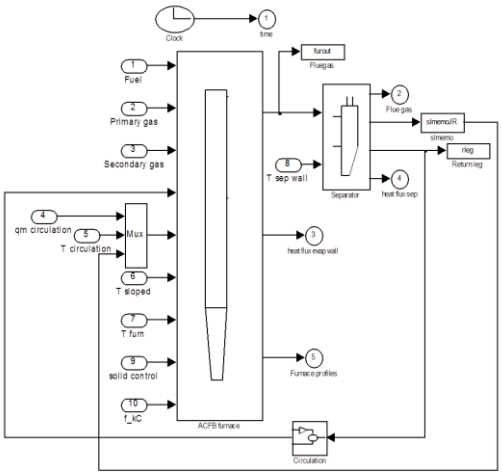

Figure 2. The hotloop model structure of the pilot plant case of this paper, containing the furnace, the separator and the return leg.

The model is nonlinear and quite large with a significant number of states, 855 for the pilot case and 660 for the industrial scale example of this paper. As a result, the model is mainly a simulator for investigating process dynamics and testing control solutions. The modeling is based on both physical and empirical approaches. A mathematical description of the model is provided in [9].

The furnace riser tube consists of 20 ideally mixed calculation elements, for which element specific mass and energy balances are solved against time with an ODE solver. A combined energy equation for gaseous and solid phase temperatures is defined, while the hydrodynamics, combustion characteristics and heat transfer inside the modules are calculated using empirical and semi-empirical correlations. The effects of the water-steam cycle are simulated through element-specific heat exchanger surface temperature parameters. The model contains no water-steam side calculations, and it is primarily used as the hotloop component in complete power plant simulators.

III. State Estimation Tool

This chapter presents the developed CFB state estimation tool and introduces the used algorithms.

A. Implementation

The CFB state estimation tool is an add-on package for the existing family of Foster Wheeler hotloop models and can readily be used for various power plant setups. The tool is utilized for estimating values for states, time-varying process parameters or "active" process inputs (e.g. fuel and gas flows). The estimates are applied as gain coefficients for model input vector elements with an initial value of 1. Several elements can also be modified with the same gain.

The aim of the tool was to utilize the original process model directly for state estimation without additional remodeling. To this end, the general model structure was implemented into the state-space representation (1).

$$\begin{cases} x(k+1) = f\big(x(k),u(k),v(k)\big) \\ y(k) = h\big(x(k),u(k)\big) + w(k) \end{cases} \quad (1)$$

The process state vector $x(k)$ is propagated into the next step $x(k+1)$ by simulating the hotloop model for the state-space timestep, starting from the initial states and applying the inputs $u(k)$. The function *"f"* thus consists of the original hotloop model nonlinear equations [9]. The probability density functions (pdf) of the measurement noise $w(k)$ and the process noise $v(k)$ are assumed to be known. The measurement equation *"h"* defines, how observations $y(k)$ are derived from $x(k)$, $u(k)$ and $w(k)$. Here, *"h"* is simply an index function that picks those elements from the hotloop model output vector that are compared to the measurements.

The aim of Bayesian state estimation is to construct a representation of the unknown state vector x through its posterior pdf $p(x_k|\tilde{Y}_k)$. $\tilde{Y}_k$ denotes all measurements y_k up to and including timestep k. The Bayesian filter provides a recursive mechanism for updating the probability of a phenomenon with evidence, i.e. updating the posterior pdf

with new output measurement data. The filter consists of prediction and update operations. In the prediction phase (2), the state posterior pdf at timestep *k-1* is propagated into a prior pdf with the model of the process dynamics.

$$\underbrace{p(x_k \mid \widetilde{Y}_{k-1})}_{prior,k} = \int \underbrace{p(x_k \mid x_{k-1})}_{processdynamics} \underbrace{p(x_{k-1} \mid \widetilde{Y}_{k-1})}_{posterior,k-1} dx_{k-1} \quad (2)$$

In the update phase (3)–(4), this result is updated with new observations to reach the posterior pdf at timestep *k*.

$$\underbrace{p(x_k \mid \widetilde{Y}_k)}_{posterior,k} = \underbrace{p(y_k \mid x_k)}_{likelihood} \underbrace{p(x_k \mid \widetilde{Y}_{k-1})}_{prior,k} \Big/ \underbrace{p(y_k \mid \widetilde{Y}_{k-1})}_{normalization} \quad (3)$$

$$p(y_k \mid \widetilde{Y}_{k-1}) = \int p(y_k \mid x_k) p(x_k \mid \widetilde{Y}_{k-1}) dx_k \quad (4)$$

The state estimation algorithm determines, how (2)–(4) is solved to gain $p(x_k \mid \widetilde{Y}_k)$. A closed form solution can be found for linear-Gaussian models with the Kalman filter, while mildly nonlinear problems can be handled by the extended Kalman filter (EKF) through linearization [7]. The hotloop tool contains two algorithms for nonlinear model state estimation. The unscented Kalman filter (UKF) is the main algorithm, while a more powerful, but also computationally demanding sampling-importance-resampling (SIR) particle filter (PF) can be used for challenging cases. Particle filters employ sequential Monte Carlo methods to describe state posterior probabilities as a set of random samples (particles), which is propagated through the system model. The approximation accuracy depends on the used amount of particles. The SIR-PF is described in [7].

B. Unscented Kalman Filter

The basic idea of the UKF is that a state variable distribution can be approximated through its mean and covariance [2,3]. The calculations rely on the unscented transform, in which a minimal set of sample points **X** ("sigma points", indicated in bold) with a mean $\bar{x}$ and a covariance P_x is used to represent an n_x-dimensional random state variable *x*. Unlike PF particles, the *2n+1* sigma points are selected according to a deterministic algorithm, which depends on the unscented transform formulation. The tool utilizes the scaled unscented transform (5)–(8) [3], while the original transform representation can be found e.g. in [2].

$$\mathbf{X}_0 = \bar{x} \quad (5)$$

$$\mathbf{X}_i = \bar{x} + \left(\sqrt{(n_x + \lambda) P_x}\right)_i, \; i=1,...,n_x \quad (6)$$

$$\mathbf{X}_i = \bar{x} - \left(\sqrt{(n_x + \lambda) P_x}\right)_i, \; i=n_x+1,...,2n_x \quad (7)$$

$$\lambda = \alpha^2 (n_x + \kappa) - n_x \quad (8)$$

In the unscented transform, the sigma points are driven through *"f"* and *"h"* in (1) to gain a cloud of transformed points **Y** (indicated in bold). The mean $\bar{y}$ is calculated as a weighted sum (9)–(12) of the transformed points, while the covariance P_y is obtained through (13). The scaled unscented transform formulation utilizes the three scaling parameters α ($0 \le \alpha \le 1$), β ($\beta \ge 0$) and κ ($\kappa \ge 0$) [3].

$$\bar{y} = \sum_{i=0}^{2n_x} W_i^{(m)} \mathbf{Y}_i \quad (9)$$

$$W_0^{(m)} = \lambda / (n_x + \lambda) \quad (10)$$

$$W_0^{(c)} = \lambda / (n_x + \lambda) + 1 - \alpha^2 + \beta \quad (11)$$

$$W_i^{(m)} = W_i^{(c)} = 1 / (2n_x + 2\lambda), \; i=1,...,2n_x \quad (12)$$

$$P_y = \sum_{i=0}^{2n_x} W_i^{(c)} \{\mathbf{Y}_i - \bar{y}\}\{\mathbf{Y}_i - \bar{y}\}^T \quad (13)$$

Equations (5)–(13) form the basis for the UKF recursive filter. In the scaled UKF [3], *x* is redefined into x^a, which contains both *x* and the system noise variables (state noise *v* and measurement noise *n*). As a result, n_x will be replaced by $n_a = n_x + n_v + n_n$ in (5)–(13). x^a is then applied to (5)–(8) to generate the sigma points $\mathbf{X}^a$ at *k*. The algorithm is initialized with (14)–(15), where $\bar{x}_0$ is the state vector initial expected value, P_0 is the initial covariance, Q is the process noise covariance and *R* is the measurement noise covariance.

$$\bar{x}_0^a = E\left[x_0^a\right] = \left[\bar{x}_0^T \quad \underline{0}^T \quad \underline{0}^T\right]^T \quad (14)$$

$$P_0^a = E\left[\left(x_0^a - \bar{x}_0^a\right)\left(x_0^a - \bar{x}_0^a\right)^T\right] = \begin{bmatrix} P_0 & \underline{0} & \underline{0} \\ \underline{0} & Q & \underline{0} \\ \underline{0} & \underline{0} & R \end{bmatrix} \quad (15)$$

Together with the process inputs *u(k)*, the sigma points are propagated through *"f"* to yield $\mathbf{X}^a_{k+1|k}$. The predicted state variable mean $\bar{x}_{k+1|k}$ is determined by applying (9) to the prior sigma points $\mathbf{X}^a_{k+1|k}$ and the weights $W^{(m)}$. Similarly, the predicted covariance $P_{k+1|k}$ is calculated with (13) by replacing $\mathbf{Y}_i$ and $\bar{y}$ with $\mathbf{X}^a_{k+1|k}$ and $\bar{x}_{k+1|k}$. Next, the transformed output points $\mathbf{Y}_{k+1}$ are gained through the measurement model "*h*". From $\mathbf{Y}_{k+1}$, (9) will give the predicted observation and (13) the respective covariance P_{yy}.

The UKF Kalman gain is determined with (16) from the cross correlation matrix P_{xy} (17) and the covariance P_{yy}.

$$K_{k+1} = P_{xy} P_{yy}^{-1} \quad (16)$$

$$P_{xy} = \sum_{i=0}^{2n_a} W_i^{(c)} \{\mathbf{X}_{k+1|k} - \bar{x}_{k+1|k}\}\{\mathbf{Y}_{k+1} - \bar{y}_{k+1}\}^T \quad (17)$$

Finally, $\bar{x}_{k+1}$ and P_{k+1} are calculated through (18).

$$\begin{cases} \bar{x}_{k+1} = \bar{x}_{k+1|k} + K_{k+1}\left(y_{k+1} - \bar{y}_{k+1}\right) \\ P_{k+1} = P_{k+1|k} - K_{k+1} P_{yy} K_{k+1}^T \end{cases} \quad (18)$$

The steps of the UKF algorithm are summarized below:

1. Define and initialize state mean vector and covariance matrix, set UKF scaling parameters.
2. Calculate sigma points $\mathbf{X}$ and corresponding weights W at timestep k.
3. Propagate each sigma point $\mathbf{X}_{k|k}$ through f (hotloop model in state-space format) to get points $\mathbf{X}_{k+1|k}$.
4. Calculate prior mean and covariance values of states: $\bar{x}_{k+1|k}$ and $P_{k+1|k}$.
5. Pass $\mathbf{X}_{k+1|k}$ through h (selection of relevant hotloop model outputs) to get $\mathbf{Y}_{k+1}$.
6. Calculate predicted observation mean/covariance.
7. Calculate cross-correlation matrix P_{xy}.
8. Calculate Kalman gain.
9. Calculate posterior mean and covariance of states, given measurements y_{k+1}.
10. Next calculation round.

The main benefits of the UKF are its estimation accuracy and ease of implementation for nonlinear systems. The estimation quality is improved compared to EKF, especially for the covariance [3]. The UKF contains only standard matrix operations and the original process model can be used directly, just like particle filters. The unscented transform makes it possible to capture high order information with a much smaller sample size than in particle filtering (amount of particles) [2]. These aspects make the UKF suitable for hotloop state estimation. One limitation of the UKF is that it doesn't apply to general non-Gaussian distributions [3].

IV. Simulations

The hotloop state estimation tool was tested through two CFB simulation cases. The aim was to illustrate the different engineering uses of the tool and to validate its functionality.

A. Pilot Case Study: Flue Gas Compositions

A measurement and dynamic simulation campaign was carried out in a pilot combustor using oxy combustion. The aim was to compare air- and oxy-firing in the CFB and to perform an initial validation of the hotloop model in oxy mode. The pilot contained the furnace, a gas-solid separator cyclone, a solids return leg, as well as flue gas recirculation and processing equipment. The oxidant was formed out of high-purity bottled O_2 and recirculated flue gas.

The state estimation case concerned a set of oxy load ramps (Fig. 3), which was conducted using a fuel blend with an approximate 70/30 mass percentage ratio of anthracite (two fractions) and petcoke. The tests showed a deviation between measured and simulated flue gas concentrations. The measured volume percentages showed variations which weren't present in the simulations and which couldn't be directly attributed to any changes in reported inputs. Moreover, the general levels of the largest concentration components CO_2 and H_2O were a bit higher in the simulations than in the measurements.

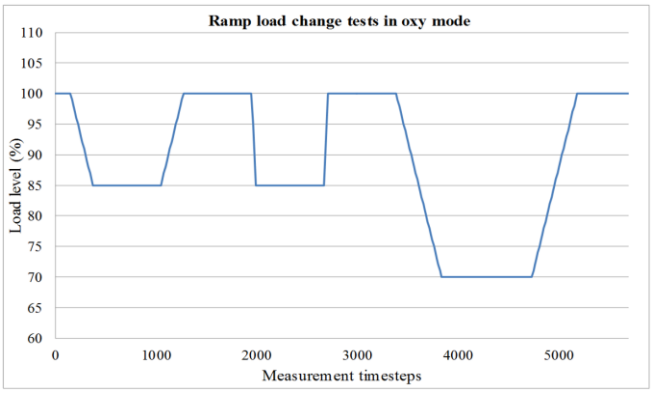

Figure 3. The boiler load levels of the oxy-firing load ramp test program.

The state estimation tool was used to investigate, whether the accuracy of the reported fuel flows and potential air leakage into the system could have caused the observed differences. The original fuel mass flows were calculated as least squares fits from fuel silo weights, effectively removing any possible higher frequency variations in the feed. Air leakage is a widely recognized problem in oxy combustion [10], as air dilutes the flue gas, and boiler overpressure can't be used. Because of the unavailability of flue gas mass flow values, a direct calculation of the air leakage amount into the boiler could not be made here. The state estimation targets were set to be the three fuel mass flows and an air leakage mass flow, which was defined as an additional input air flow to the combustion side. The air leakage was given a nominal value significantly below the primary and secondary input gas flows. The flue gas CO_2 and O_2 volume percentages were used as the measurements for the state estimation.

The estimation results in Figs. 4–5 displayed a good agreement between measurements and simulations, when the small flue gas concentration changes and the general levels of the larger components were considered. Notably, the flue gas moisture content was also on target, although it hadn't been used for state estimation. This was especially apparent after the FTIR moisture sensor cleaning at timestep 900.

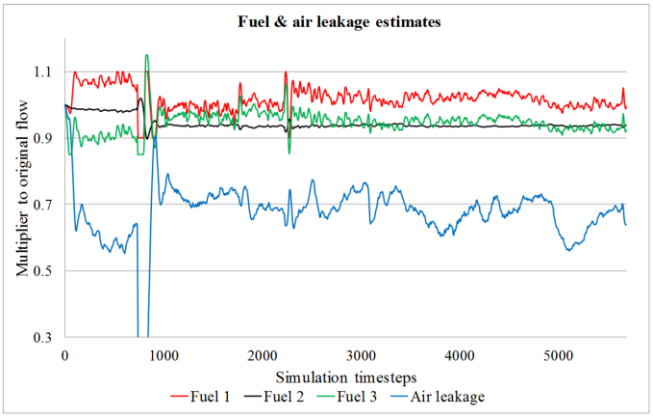

Figure 4. Estimated fuel mass flow (3 parameters) and air leakage gain coefficients of the pilot oxy load ramp test program.

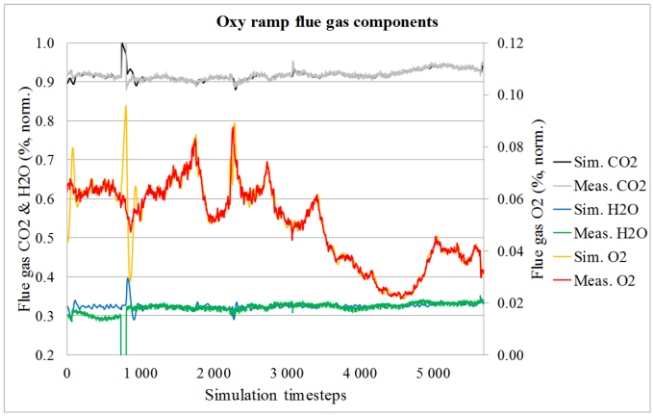

Figure 5. Normalized flue gas vol-% outputs (CO_2, H_2O and O_2) of the oxy load ramp state estimation simulations and the pilot scale measurements. The values were normalized with the concentration maxima.

The estimates offered a plausible explanation for the differences between the simulations and the measurements. It was also apparent that adjusting only the fuel flows was not enough to achieve the measured O_2 and CO_2 values. The estimated parameter values were deemed to be realistic, as both the fuel flow corrections and the air leakage remained reasonably constant, and the fuel corrections were small enough. The air ingress into the boiler was also significantly smaller than the actual primary and secondary gas inputs.

B. Industrial Case Study: Heat Transfer & Fuel Moisture

Here, tests with a full scale air-fired industrial boiler with one input fuel fraction (coal-firing) were examined. The measurement campaign consisted of the three test sets below. From these, the reactivity test data was previously utilized in [7] for SIR-PF and initial UKF state estimation testing.

1. Reactivity tests – stepwise changes in the fuel flow.
2. Primary tests – stepwise changes in the primary air:

   + 6 % to primary input air flow at timestep 230.

   – 6 % to primary input air flow at timestep 650.
3. Load tests: stepwise changes in fuel and air flows:

   – 8 % to input fuel and air flows at timestep 310.

   + 8 % to input fuel and air flows at timestep 540.

The dynamic tests showed differences between measured and modeled dense bed furnace temperatures and flue gas O_2 contents. Temperature differences could be seen both for the general temperature level and for smaller variations, while the measured O_2 general level matched the simulations better. Based on process knowledge and sensitivity analyses, state estimation was implemented to determine one furnace heat transfer coefficient and the fuel moisture content, using the furnace temperature and the flue gas O_2 as outputs. Tuning of heat transfer coefficients is a common operation in hotloop model synthesis and it's often done iteratively. The variation in the fuel H_2O content is an acknowledged control challenge in solid fuel combustion, mainly due to the difficulties related to online moisture measurements [11], fuel quality variations and co-firing of different fuels.

Figs. 6–7 display the estimated parameters and outputs of the load steps, while the primary test results can be seen in Figs. 8–9. There was mostly a good agreement between measurements and simulations and the results corresponded to the reactivity tests in [7]. The simulated temperature settled on the average level of the measurements, and the smaller variations in the temperature and the flue gas O_2 could be captured in most cases. For both tests here and the reactivity tests, the heat transfer coefficient settled between 1.4–1.6. As a result, the dense bed heat transfer coefficient should be multiplied by 1.5 to improve modeling accuracy.

The state estimation produced better results for the primary tests than for the load tests. This applied especially to load change temperatures, and at 540, the temperature was even corrected in the opposite direction than the measured output. The reduced performance of the estimation can be related to the instantaneous changes in all inputs, which cause more significant alternations in the heat generation than just primary air steps. This is supported by the good load ramp simulation results in Figs. 4–5. However, there might also be a need to investigate other parameters and outputs, as there may have been unobserved changes in the process that aren't covered by the selected variables of this work. Indeed, load level changes might not be visible enough in temperatures close to the furnace grate or the flue gas O_2.

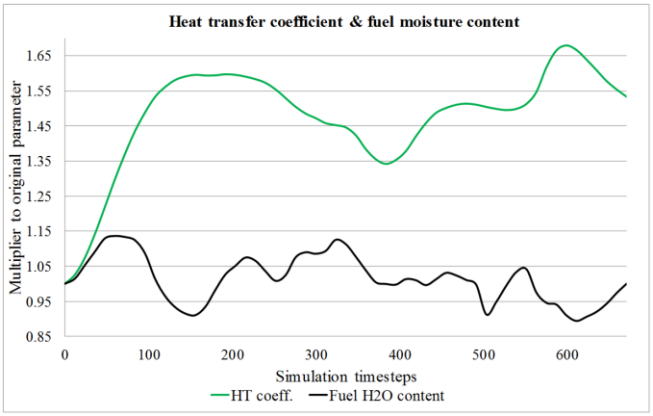

Figure 6. Estimated furnace heat transfer (HT) coefficient and fuel moisture content gain coefficient for the industrial load step tests.

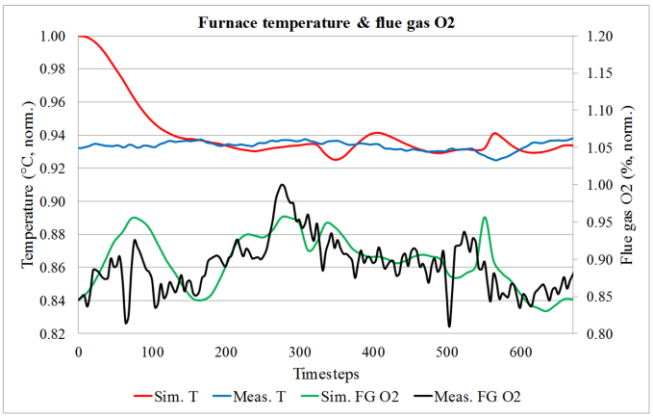

Figure 7. Normalized dense bed furnace temperatures (T) and flue gas O_2 w-% outputs of the load step state estimation simulations and industrial measurements. The outputs were normalized with the respective maxima.

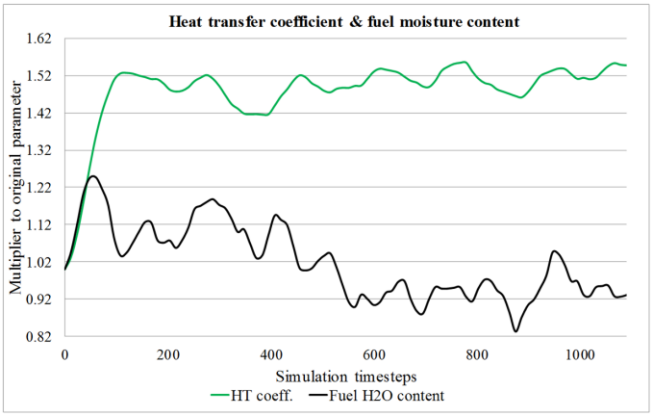

Figure 8. Estimated furnace heat transfer (HT) coefficient and fuel moisture content gain coefficient for the industrial primary air tests.

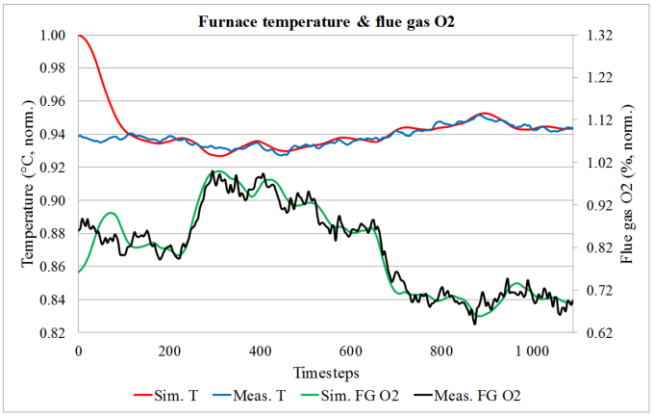

Figure 9. Normalized dense bed furnace temperatures (T) and flue gas O_2 w-% outputs of the primary air state estimation simulations and industrial measurements. The outputs were normalized with the respective maxima.

The fuel moisture content changes were quite realistic and the parameter window was approximately the same for all tests. The primary tests showed slightly higher moisture values at the start, suggesting a gradual change in fuel quality. It could be stated that a constant fuel moisture content assumption was not enough for accurate hotloop modeling. On a whole, the estimated heat transfer coefficient and fuel moisture content values could successfully be used to explain the differences between measurements and simulations. Moreover, the UKF proved to have a significant computational advantage over the current implementation of the SIR-PF in the tool, as comparable results to the PF were obtained in a much shorter calculation time with the UKF.

V. Conclusion

A Bayesian state estimation tool for circulating fluidized bed hotloop models was constructed and tested in this paper, with the scaled unscented Kalman filter as the main algorithm. The tool proved to be readily useable for various CFB model versions and design problems, as was showcased by two case study setups. The examples illustrated the applicability of state estimation to different tasks: The pilot oxy combustion case concentrated on model validation, while the industrial case investigated fuel quality variations and heat transfer changes during the boiler operation. Both examples yielded good results concerning the outputs and the estimates. Furthermore, Bayesian state estimation hasn't previously been applied to solve the modeling and analysis problems presented in this work. The computational performance of the UKF was good, and the results were comparable to a heavier particle filtering approach. The algorithm was also directly applicable to the original hotloop model without additional modeling, e.g. linearization.

Future work with the state estimation tool concerns applying it to various boiler models and tasks in order to assess its performance. The UKF framework of the tool can be developed further to increase its performance and accuracy. One particular topic of interest would be the possibility to gain rough estimates of time-varying heat transfer coefficients and heat exchanger surface temperatures during model tuning based on hotloop MW targets.

Acknowledgment

The authors gratefully acknowledge the cooperation with the Lappeenranta University of Technology (LUT). Parts of the work have received funding from the Graduate School in Chemical Engineering (GSCE).

References

[1] E. Ikonen and K. Najim, *Advanced Process Identification and Control*. New York (NY): Marcel Dekker Inc., 2002, 328 p.

[2] S. J. Julier and J. K. Uhlmann, "A New Extension of the Kalman Filter to Nonlinear Systems," in *Proc. AeroSense: 11th Int. Symp. Aerosp./Def. Sens., Simul. Controls, Vol. Multi Sens. Fusion, Track. Resour. Manag. II*, Orlando (FL), 1997, pp. 182–193.

[3] R. van der Merwe, A. Doucet, N. de Freitas and E. Wan, "The Unscented Particle Filter," Technical report CUED/F-INFENG/TR 380, Cambridge Univ. Eng. Dept., Cambridge, UK, 2000, 46 p.

[4] J. Park., "System Identification and Control of the Standpipe in a Cold Flow Circulating Fluidized Bed," Ph.D. dissertation, Lane Dept. Comp. Sci. Elect. Eng., West Virginia Univ., Morgantown, WV, 2004.

[5] A. A. Jalali, J. Park, P. Famouri, R. Turton and E. J. Boyle, "H_∞ based state estimation on standpipe of a cold flow circulating fluidized bed," in *Proc. IEEE Int. Conf. Syst. Man Cybern., Vol. 3*, Washington D.C., 2003, pp. 2320–2325.

[6] L. Sun, J. Dong, D. Li and Y. Zhang "Model-Based Water Wall Fault Detection and Diagnosis of FBC Boiler Using Strong Tracking Filter," *Math. Probl. Eng.*, vol. 2014, ID 504086, 8 p., Apr. 2014.

[7] E. Ikonen, J. Kovács and J. Ritvanen, "Circulating Fluidized Bed Hot-Loop Analysis, Tuning, and State-Estimation Using Particle Filtering," *Int. J. Innov. Comput. Inf. Control*, vol. 9, no. 8, pp. 3357–3376, Aug. 2013.

[8] M. Hultgren, E. Ikonen and J. Kovács, "Oxidant control and air-oxy switching concepts for CFB furnace operation," *Comput. Chem. Eng.*, vol. 61, pp. 203–219, Feb. 2014.

[9] J. Ritvanen, J. Kovács, M. Salo, M. Hultgren, A. Tourunen and T. Hyppänen, "1-D Dynamic Simulation Study of Oxygen Fired Coal Combustion in Pilot and Large Scale CFB Boilers," in *Proc. 21st Int. Conf. Fluid. Bed Combust., Vol. 1*, Naples, 2012, pp. 72–79.

[10] M. B. Toftegaard, J. Brix, P. A. Jensen, P. Glarborg and A. D. Jensen, "Oxy-fuel combustion of solid fuels," *Prog. Energy Combust. Sci.*, vol. 36, no. 5, pp. 581–625, Oct. 2010.

[11] J. Kortela and S.-L. Jämsä-Jounela, "Fuel-quality soft sensor using the dynamic superheater model for control strategy improvement of the BioPower 5 CHP plant," *Int. J. Electr. Power Energy Syst.*, vol. 42, no. 1, pp. 38–48, Nov. 2012.